Journal of Hazardous Materials 248–249 (2013) 285–294

Contents lists available at SciVerse ScienceDirect

Journal of Hazardous Materials

journal homepage: www.elsevier.com/locate/jhazmat

Preparation, characterization and adsorption properties of a novel 3-aminopropyltriethoxysilane functionalized sodium alginate porous membrane adsorbent for Cr(III) ions

Jian Hua Chen*, Hai Tao Xing, Hong Xu Guo, Guo Ping Li, Wen Weng, Shi Rong Hu

Department of Chemistry and Environmental Science, Zhangzhou Normal University, Zhangzhou 363000, China

HIGHLIGHTS

- The APTEOS/SA has been successively applied for adsorption removal of Cr(III) ions.
- The APTEOS/SA exhibited excellent uptake capacity of 1.73 mmol/g.
- The APTEOS/SA could be used conveniently.
- The APTEOS/SA could be reused with little loss of adsorption capacity.
- The adsorption rate was fast and adsorption equilibrium was obtained within 50 min.

ARTICLE INFO

Article history:
Received 7 November 2012
Received in revised form
17 December 2012
Accepted 17 January 2013
Available online xxx

Keywords:
Sodium alginate
Membrane
3-Aminopropyl-triethoxysilane
Adsorption
Cr(III)

ABSTRACT

In this study, we prepared 3-aminopropyl-triethoxysilane (APTEOS) functionalized sodium alginate (SA) porous membrane adsorbent (APTEOS/SA) and tested its adsorption performance for removing of Cr(III) ions. The physico-chemical properties of the pristine and Cr(III) ions loaded APTEOS/SA were investigated by FT-IR, SEM-EDX, TG, AFM, and contact angle goniometer methods. To investigate the adsorption kinetics of Cr(III) ions onto this newly developed APTEOS/SA, we performed a batch of experiments under different adsorption conditions: solution pH, adsorbent dose, initial Cr(III) ion concentration, adsorption temperature, and contact time. The APTEOS/SA exhibited an encouraging uptake capacity of 90.0 mg/g under suitable adsorption conditions. To study the mechanism of adsorption process, we examined the Lagergren pseudo-first-order and pseudo-second-order kinetic model, the intra-particular diffusion model, and the Crank model. Kinetics experiments indicated that the pseudo-first-order model displayed the best correlation with adsorption kinetics data. The Crank model showed that the intra-particle solute diffusion was the main rate-controlling step. Furthermore, our adsorption equilibrium data could be better described by the Freundlich equation. We also carried out consecutive adsorption–desorption experiments eight times to show that the APTEOS/SA has encouraging adsorption–desorption efficiencies. The results indicates that the prepared adsorbent is promising for using as an effective and economical adsorbent for Cr(III) ions removal.

1. Introduction

In the past decades, with the rapid increase in global industrial activities and mining activities, heavy metal pollution has caused serious environmental and public health problems in many places worldwide [1,2]. One of the most toxic metal ions endangering human life is chromium [3–6]. Cr(III) ion compounds are widely used in modern industries, such as leather making, textile dyeing, wood preservation, metal finishing and petroleum refining [7–10], which inevitably results in a large quantity of Cr(III) ions contaminated industrial effluents. Waters containing a high concentration of Cr(III) ions are extremely harmful to human beings because they are non-biodegradable in living tissues and would induce toxic and carcinogenic health effects on humans [11,12]. Therefore, the methods for removal of Cr(III) from wastewater with high efficiency and low cost are urgently needed.

The conventional methods used to remove heavy metal ions from wastewater include chemical precipitation, ion exchange, chemical reduction and membrane separation [13–16]. However, these methods are not widely practical due to their high operating costs and problems in the disposal of residual metal sludge. Removal of Cr(III) ions from wastewater by adsorption has been investigated by many researchers [17–21]. The main advantages of the adsorption are a recovery of the heavy metal, high selectivity,

* Corresponding author. Tel.: +86 596 2591445; fax: +86 596 2520035.
E-mail address: jhchen73@126.com (J.H. Chen).

0304-3894/$ – see front matter © 2013 Elsevier B.V. All rights reserved.
http://dx.doi.org/10.1016/j.jhazmat.2013.01.042

less sludge volume produced, simplicity of design and the meeting of strict discharge specification. An efficient adsorptive material should consist of an insoluble porous matrix and some suitable active groups that can interact with heavy metal ions [22,23].

In recent years, increased attention has been focused on the use of abundantly naturally available and reusable low cost geomaterials and biomaterials, such as, phillipsite [24], clinoptilolite-bearing volcanoclastic deposits [25], natural zeolites [26], cellulose [27,28], starch [29], dextran [30,31] and chitosan [32–34] for removing heavy metal ions from wastewater or as cation exchanger. Compared with other traditional treatment processes, heavy metal adsorption using geomaterials and biomaterials can reduce total capital cost greatly and make the adsorption process more environmental friendly and more technical feasibly. Sodium alginate (SA) is naturally occurring polysaccharides obtained mainly from marine brown algae belonging to the phaeophyceae, and is composed of two monomeric units, h-D-mannuronic acid and a-L-guluronic acid [35,36]. Sodium alginate, for its good membrane forming properties and high activity with carbonyl and hydrogen groups on its chain which are excellent functional groups for anchoring heavy metals, has been attracted considerable attention currently [37–39]. However, in many cases, these biomaterials are soluble in aqueous solution and usually do not exhibit satisfied adsorption performance for target heavy metals. As a result, their modification is needed to enhance their adsorption capacity [29,40–42].

Based on remark above, in this study, a novel porous membrane adsorbent (APTEOS/SA) was prepared by functionalizing SA with 3-aminopropyl-triethoxysilane (APTEOS) and using silica gel as a porogen, and used for adsorption removal of Cr(III) ions from wastewater. To investigate the effects of operating factors on the adsorption capacity of the APTEOS/SA for Cr(III) ions, we carried out a batch of adsorption experiments under various conditions: solution pH, adsorbent dose, initial Cr(III) ion concentration, adsorption temperature and contact time. By testing various adsorption and kinetics models to fit our experimental data, we also studied the adsorption kinetics and isotherms of the APTEOS/SA for Cr(III) ions. The desorption and reusability of the APTEOS/SA for Cr(III) ions were also investigated.

2. Experimental

2.1. Materials and analytical method

Sodium alginate (1.05–1.15 Pa s at 10 mg/L, Xilong Chemical Co. Ltd., China), Chromium(III) nitrate nonahydrate ($Cr(NO_3)_3.9H_2O$% ≥99.0, Xilong Chemical Co. Ltd., China), Sodium hydroxide (NaOH% ≥96.0, Xilong Chemical Co. Ltd., China), γ-aminopropyltriethoxysilane (0.946 g/mL at 25 °C, Yaohua Chemical Co. Ltd., China), silica gel (300–400 m^2/g, Yantai Jiangyou Guijiao Co. Ltd., China) were purchased from Shanghai Chemical Reagent Store (Shanghai, China). All of them are of analytical grade and used without further purification.

A stock solution of 100 mg/L of Cr(III) ions was prepared by dissolving 1.5420 g of $Cr(NO_3)_3{\cdot}9H_2O$ in 2000 mL distilled water. The desired Cr(III) ion solutions were prepared by diluting of the stock Cr(III) ion solution. Solutions of 0.1 M NaOH and HCl were used for adjusting the solution pH. The chromium concentration was spectrophotometrically measured using standard procedure at λ = 420 nm [43], and the errors were no more than 2.5%.

2.2. Preparation of porous membrane adsorbent APTEOS/SA

Six grams of SA was dissolved in 400 mL deionized water following with the addition of 0.048 g silica gel. To the solution, 1 mL of aqueous 1 M HCl and 6 mL of APTEOS were added dropwise under vigorous stirring with a blender (DSX-120, Hangzhou Electric Instrument Co. Ltd., China) at a speed of 1000 rpm. The resulted solution was cast onto a glass plate (12 cm × 12 cm), and then dried in an oven at 70 °C for 120 min. The dried membranes were carefully peeled off and further dried in an oven at 70 °C for 240 min. Finally, the obtained membranes were immersed in a 1.0 M HCl solution for 60 min to remove the porogen silica gel, and then immersed in deionized water again for one day. The resulted membranes were dried in an oven at 70 °C for 120 min, then, stored in a desiccator for further experiments.

2.3. Membrane characterization

FT-IR spectra of the pristine and Cr(III) ions loaded APTEOS/SA were scanned in the range from 4000 to 400 cm^{-1} by means of ATR-FTIR with an accumulation of 16 scans, resolution of 0.4 cm^{-1}, on a Nicolet-740.

The surface morphology of the pristine and Cr(III) ions loaded APTEOS/SA were also characterized by SEM (Hitachi S-4800), equipped with an energy dispersive X-ray spectroscope, which was operated at EHT = 4.0 kV.

A CSPM-5500 scanning probe microscope (AFM, Benyuan, China) was used to carry out the morphological characterization of the pristine and Cr(III) ions loaded APTEOS/SA, operated in tapping mode. Tapping mode cantilevers (Tap300Al, Budget Sensors) with a spring constant of 40 N/m were used throughout the imaging.

The thermal properties of the pristine and Cr(III) ions loaded APTEOS/SA were analyzed using thermogravimetric analysis (Netzsch TG209 F1). Accurately weighted (8 mg) sample was placed into aluminum cup and heated from room temperature to 900 °C at a constant heating rate 10 °C/min under constant nitrogen purging at 20 mL/min.

Water contact angle as well as the surface energy of the pristine and Cr(III) ions loaded APTEOS/SA were measured by the pendant drop method using a contact angle meter (SL200B, SOLON TECH, Shanghai, China), equipped with a CAST2.0 software, at 25 ± 1 °C, under 70 ± 1% relative humidity condition. All reported values were the average of eight measurements taken at different location of the same membrane surface.

2.4. Adsorption procedure

The stock Cr(III) ions solution with concentration of 100 mg/L was prepared by using $Cr(NO_3)_3{\cdot}9H_2O$ as a source of Cr(III) ions. Experimental solutions of the desired concentrations were obtained by successive dilution. The desired solutions pH was adjusted by adding either 0.1 M NaOH or HCl solution. Adsorption experiments were carried out in a 500 mL volumetric flask using 250 mL Cr(III) ions solution as well as the required amount of adsorbent. The flasks were placed on an orbital shaker running at 120 rpm at 25 ± 1 °C until equilibrium was obtained. Five milliliters of the sample was drawn at regular intervals for residual concentration testing. All the experiments were performed in triplicate and the average was taken for subsequent calculations.

The adsorption capacity of the adsorbent was evaluated by using the following expression:

$$q_t = \frac{(C_0 - C_t)V}{m} \quad (1)$$

where q_t is the mass of Cr(III) ions adsorbed per unit mass of the adsorbent (mg/g), V is the volume of the solution (L), m is the mass of the adsorbent (g), and C_0 and C_t are the concentration of Cr(III) ions in the initial aqueous solution and in the aqueous solution after adsorption for t min (mg/L), respectively.

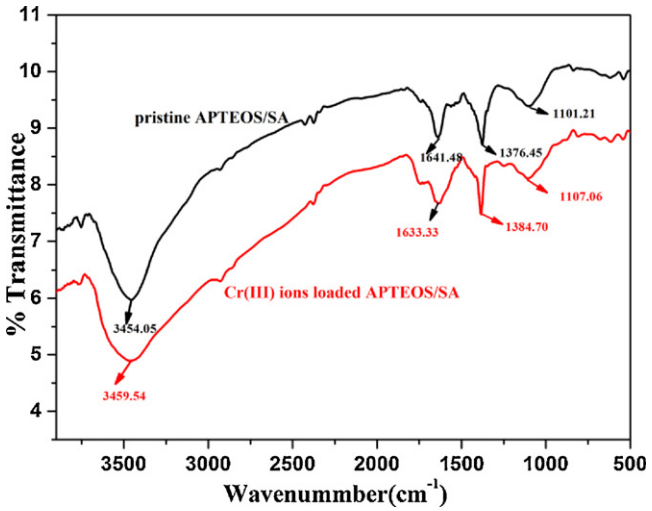

Fig. 1. FT-IR spectra of: (a) pristine APTEOS/SA; (b) Cr(III) ions loaded APTEOS/SA (resolution of 0.4 cm^{-1}).

2.5. Desorption of heavy metal ions and membrane reusability

Desorption of Cr(III) ions was carried out using 1.0 M HCl as a desorbing agent. The Cr(III) ions loaded APTEOS/SA membrane samples were placed in a 250 mL desorption medium at 25 °C, with a shaking speed of 120 rpm for 120 min. The membrane samples were washed with deionized water several times and subjected again to adsorption/desorption process for eight cycles.

3. Results

3.1. Characterization of pristine and Cr(III) ions loaded APTEOS/SA

3.1.1. FT-IR analysis

FT-IR spectra of the pristine and Cr(III) ions loaded APTEOS/SA are presented in Fig. 1. When both the spectra are compared, the following changes are observed. The spectrum of the pristine APTEOS/SA exhibit a broad absorption band around 3454.05 cm^{-1} corresponding to O—H stretching vibrations of the hydroxyl groups and N—H stretching vibrations of the amide groups [44] is shifted to 3459.54 cm^{-1} after adsorption of Cr(III) ions, which may be ascribed to the complexation of —OH and amide groups with Cr(III) ions. The absorption band appearing at 1641.48 cm^{-1} has shifted to 1633.33 cm^{-1}, which may be attributed to the complexation of carboxylic group with Cr(III) ions [45,46]. The peaks observed at 1376.45 and 1101.21 cm^{-1} have shifted to 1384.70 and 1107.06 cm^{-1} which may also be attributed to the interaction of amino group with Cr(III) ions.

3.1.2. SEM images

The SEM images of the pristine and Cr(III) ions loaded APTEOS/SA are shown in Fig. 2(a) and (b), respectively. The SEM images clearly show that the reaction of Cr(III) ions with the APTEOS/SA made the surface of the APTEOS/SA more roughness and protrusion. Meanwhile, the surface characteristic of the Cr(III) ions loaded and the pristine APTEOS/SA were also investigated using an energy dispersive X-ray (EDX), and the results are shown in Fig. 3(a) and (b), respectively. From Fig. 3, one can find that the characteristic signal of Cr(III) (5.45 wt%) could only be observed in Fig. 3(a), which may be ascribed to the adsorption of Cr^{3+}, $Cr(OH)^{2+}$ and $Cr(OH)_2^{+}$ (refer to Section 3.2) on the APTEOS/SA.

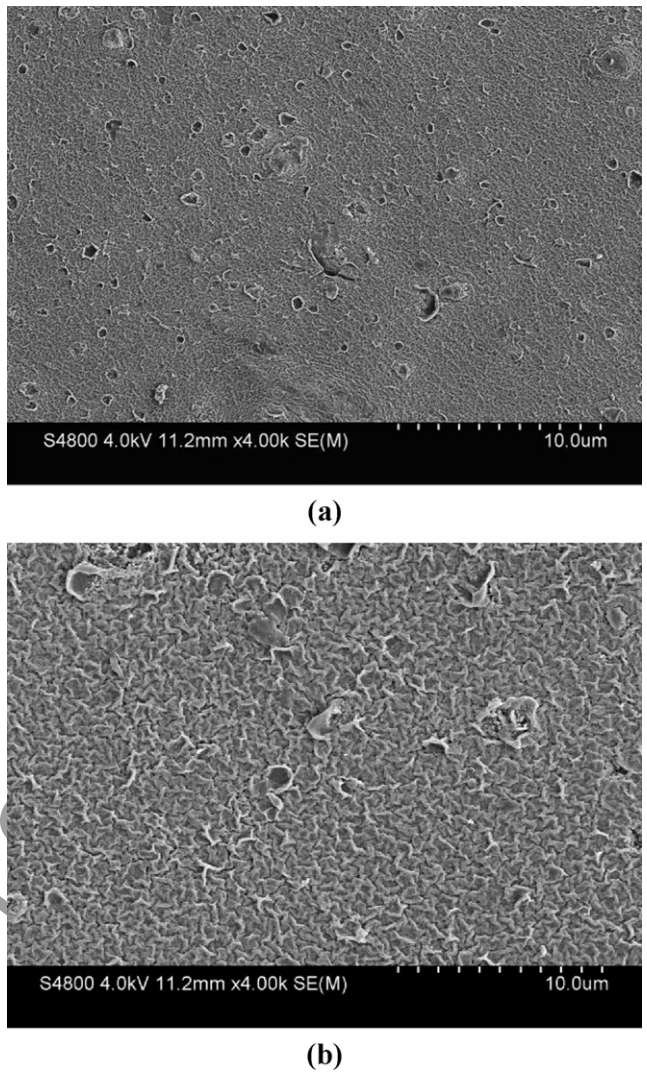

Fig. 2. SEM images of: (a) pristine APTEOS/SA; (b) Cr(III) ions loaded APTEOS/SA (magnification 4000×).

3.1.3. Surface three-dimensional morphology analysis

AFM is one of the most useful tools for investigating nanoscale surface topographies of the membrane. This technique gives a three-dimensional image for offering information concerning changes in the surface roughness of a membrane adsorbent. Fig. 4 shows the AFM images for the pristine and Cr(III) ions loaded APTEOS/SA with a scope of 4000 nm × 4000 nm, where the dark color zones represent depressions and light color regions correspond to the highest points on the surface of the membrane. The adsorption of Cr(III) ions made the surface of the APTEOS/SA more coarse. The calculated roughness average (R_a) of the surfaces for the APTEOS/SA before adsorption was 8.15 nm. This value increased to 27.6 nm after the Cr(III) ions were adsorbed.

3.1.4. Thermal properties analysis

Thermal properties of the pristine and Cr(III) ions loaded APTEOS/SA are presented in Fig. 5(a) and (b), respectively. As for pristine APTEOS/SA, the first weight loss stage between 30 °C and 131 °C was 6.12 wt%, which is associated with the evaporation of water adsorbed on the surface of the APTEOS/SA; the second weight loss stage between 176 °C and 487 °C was 45.67 wt%, which was attributed to the decomposition of $—NH_3^+$, $—COO^-$ and —OH groups of the APTEOS/SA; and the next one higher than 521 °C can be attributed to the main chain depredation; finally, when the

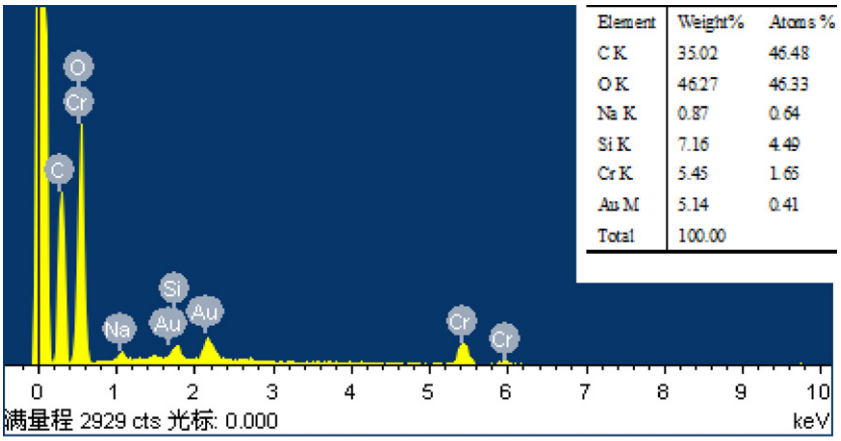

(a)

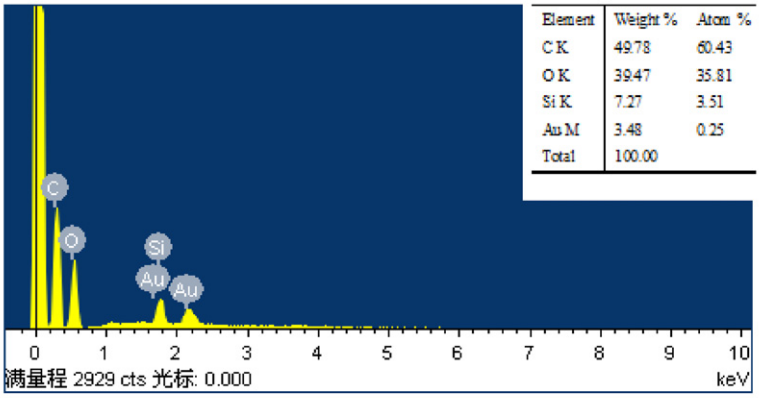

(b)

Fig. 3. Energy dispersive X-ray (EDX) analysis of: (a) pristine APTEOS/SA; (b) Cr(III) ions loaded APTEOS/SA (magnification 4000×).

temperature was 810 °C the residue was about 25.12 wt% which can be mainly ascribed to SiO_2 (the calculation value from experiment data 16.72 wt%, EDX testing value, 15.6 wt%), the decomposing production of the APTEOS. From Fig. 5, we can find that both the thermal properties of the pristine and Cr(III) ions loaded APTEOS/SA are similar; however, the difference of both the residues was 9.89 wt% when the temperature was 900 °C. This can mainly be attributed to the adsorption of chromium species (such as Cr^{3+}, $Cr(OH)^{2+}$ and $Cr(OH)_2{}^{+}$) onto the APTEOS/SA, their decomposing production were Cr_2O_3 (the value calculated for experiment data 8.36 wt%, EDX testing value Cr_2O_3 7.97 wt%).

3.1.5. Water contact angle and surface energy test

The result of the water contact angle and surface energy test of the adsorbent indicated that before Cr(III) ions adsorption, the water contact angle and surface energy of the adsorbent were 32.45° and 41.54 J/m^2, however, after Cr(III) ions adsorption, the water contact angle and surface energy of the adsorbent were 63.91° and 33.05 J/m^2, respectively.

3.2. Effects of solution pH on adsorption

The effect of solution pH on adsorption was studied for the solution pH in the range of 2.0–7.0. Effect of solution pH on the adsorption capacity of the APTEOS/SA for Cr(III) ions was significant, as indicated in Fig. 6. Adsorption capacity, q_e obtained the maximum at solution pH 6.0. This behavior can be explained by the change in the ionic state of the amine and carboxyl function groups in the adsorbent [47]. When the solution pH is low, functional groups were protonated. As a result, Cr(III) ions uptake capacity decreased. Meanwhile, chromic ion species exist in acidic solution as bulky hydrated species ($Cr(H_2O)_6{}^{3+}$); this ion was too large to enter in the micro-pores of the APTEOS/SA [5]. When the solution pH was increased gradually, amine and carboxyl function groups were deprotonated and Cr^{3+} ion (principal species at low pH value) can be bound to negatively charged groups by electrostatic attraction. A further increasing in the solution pH results in a decreasing of Cr^{3+} concentration and other species become important, such as $CrOH^{2+}$ and monovalent $Cr(OH)_2{}^{+}$ [5], which diminished Cr(III) ions adsorption at solution pH higher than 6.0. Meanwhile, precipitate could occur at a higher solution pH. To make sure the maximum removal efficiency as well as to avoid precipitation of Cr(III) ions, all the following experiments were carried out at solution pH 6.0.

3.3. Effects of initial Cr(III) ions concentration on adsorption

In batch adsorption processes, initial metal ion concentration provides an important driving force to overcome the mass transfer resistance of Cr(III) ions between the aqueous solution and the APTEOS/SA surface. As a result, the amount of Cr(III) ions adsorbed was expected to be higher with a higher initial metal ions concentration, hence improving the adsorption process. From Fig. 7, we can find that when the initial Cr(III) ions concentration increased from 32 to 104 mg/L, the uptake capacity of the APTEOS/SA for Cr(III) ions increased from 16.6 to 81.6 mg/g. This can be explained from two aspects: firstly, higher initial Cr(III) ions concentration increased driving force to overcome the mass transfer resistance of Cr(III) ions between the aqueous and solid phases resulting in higher

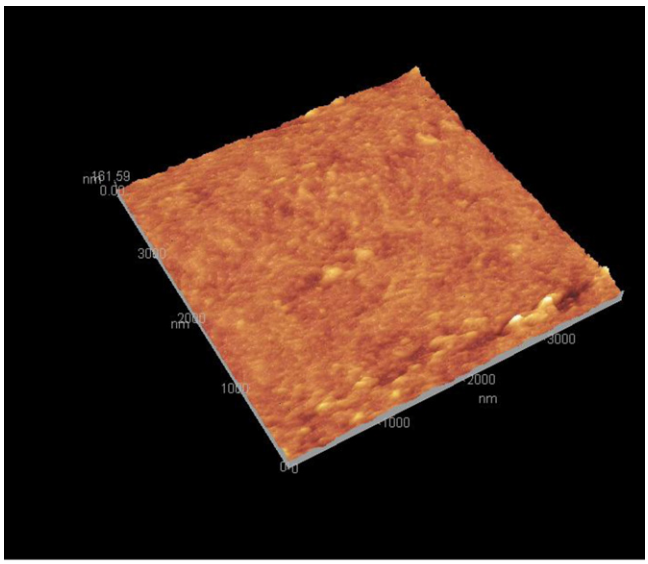

Fig. 4. AFM images of: (a) pristine APTEOS/SA; (b) Cr(III) ions loaded APTEOS/SA (tapping mode; spring constant 40 N/m).

probability of collision between the Cr(III) ions and the APTEOS/SA, and secondly, the increase of Cr(III) ions uptake capacity of the APTEOS/SA for Cr(III) ions with increasing initial Cr(III) ions concentration may also be attributed to a more intensity interaction between the Cr(III) ions and the APTEOS/SA.

3.4. Effects of adsorbent dose on adsorption

The effect of adsorbent dosage on adsorption results presented in Fig. 8 indicated that when the adsorbent dose was increased from 0.08 to 0.84 g/L, Cr(III) ions uptake capacity of the APTEOS/SA decreased drastically from 89.93 to 35.31 mg/g. It can be attributed to the fact that when more adsorbent dose was added some of the adsorption sites remain unsaturated during the adsorption process, and thus results in a lesser adsorption capacity.

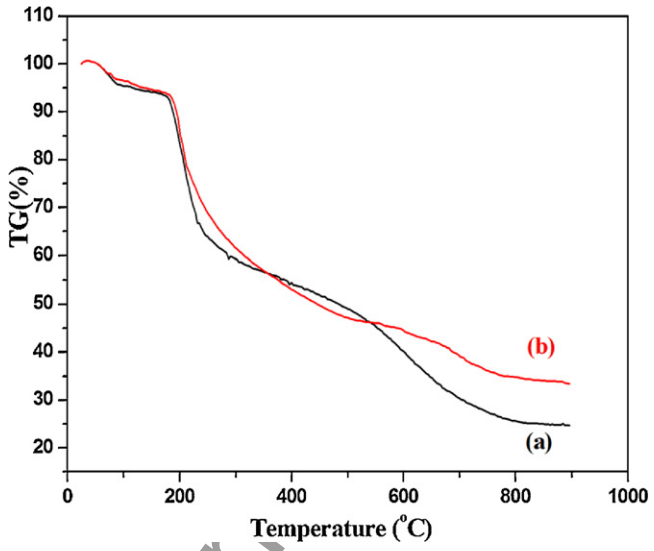

Fig. 5. Thermal-gravimetric curves of: (a) pristine APTEOS/SA; (b) Cr(III) ions loaded APTEOS/SA (heating rate 10 °C/min; nitrogen purging 20 mL/min).

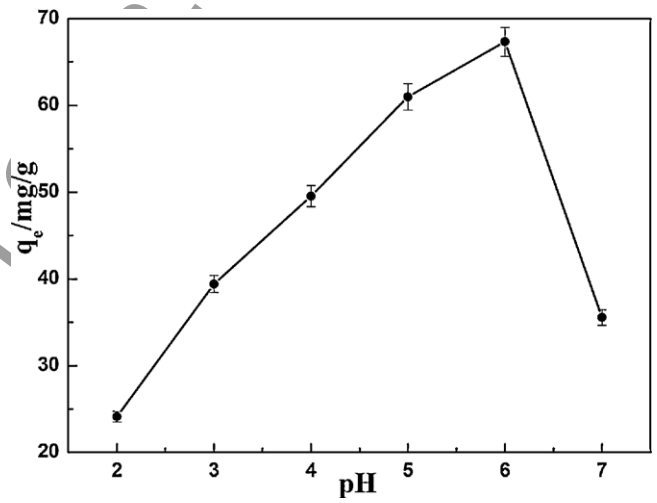

Fig. 6. Effects of solution pH on adsorption capacity: Cr(III) ions concentration 63 mg/L; adsorbent dosage 0.2 g/L; temperature 25 °C; speed agitation 120 rpm; and time 50 min.

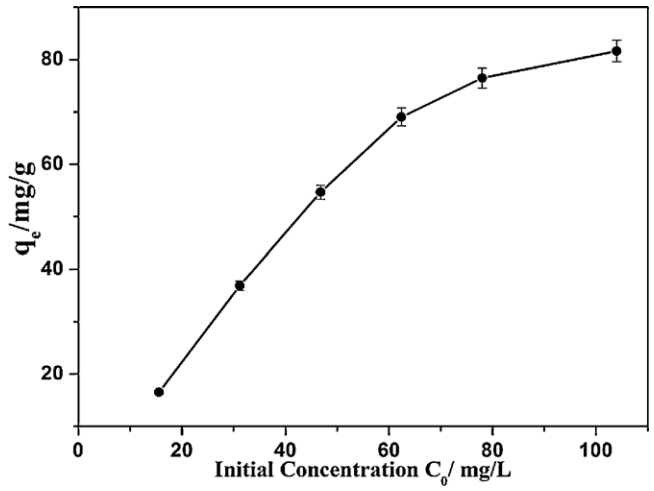

Fig. 7. Effects of initial Cr(III) ions concentration on adsorption capacity: adsorbent dosage 0.2 g/L; temperature 25 °C; pH 6.0; speed agitation 120 rpm; and time 50 min.

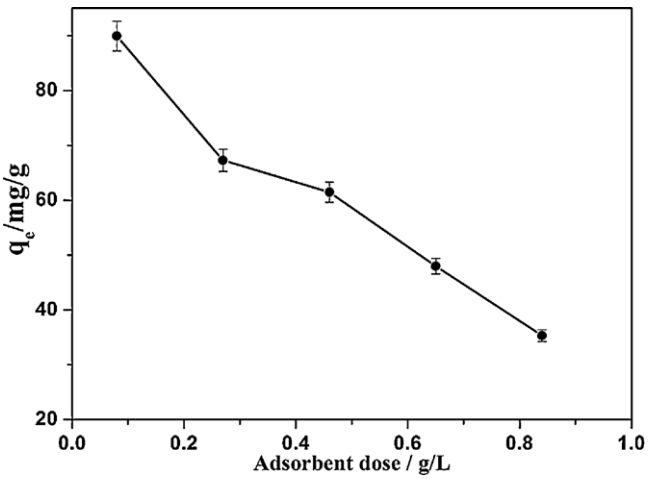

Fig. 8. Effects of adsorbent dose on adsorption capacity: Cr(III) ions concentration 63 mg/L; temperature 25 °C; pH 6.0; and speed agitation 120 rpm; and time 50 min.

3.5. Effects of temperature on adsorption

It has been recognized that the adsorption of heavy metal ions from an aqueous solution by adsorbent is affected by the temperature. An increase in temperature is known to increase the diffusion rate of the adsorbate molecules across the external boundary layer and within the pores of the porous adsorbent. Furthermore, changing the temperature will modify the equilibrium capacity of the adsorbent for a particular adsorbate. The effects of temperature on the adsorption capacity of the APTEOS/SA for Cr(III) ions are presented in Fig. 9. It indicated that the adsorption capacity increased slowly with a higher temperature. The increase in Cr(III) adsorption capacity of the APTEOS/SA with higher temperature indicated the endothermic nature of the adsorption process. The increase in Cr(III) uptake capacity with a higher temperature could be explained from two aspects: firstly, as the temperature rises, the diffusion of Cr(III) ions becomes much easier into the pore of APTEOS/SA because of the increase in the degree of swelling. As a result, the adsorption capacity of the APTEOS/SA for Cr(III) ions increases; secondly, bond rupture of the functional groups on the adsorbent surface at an elevated temperature may increase the number of active adsorption sites, which may also lead to an enhanced adsorption capacity of the adsorbent.

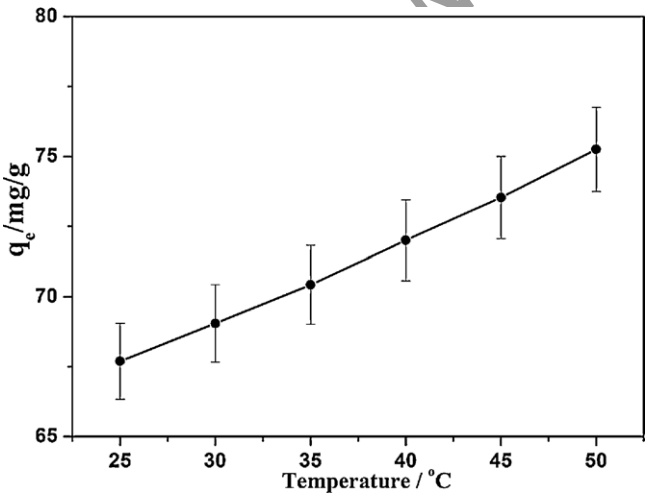

Fig. 9. Effects of temperature on adsorption capacity: adsorbent dose 0.2 g/L; Cr(III) ions concentration 63 mg/L; pH 6.0; speed agitation 120 rpm; and time 50 min.

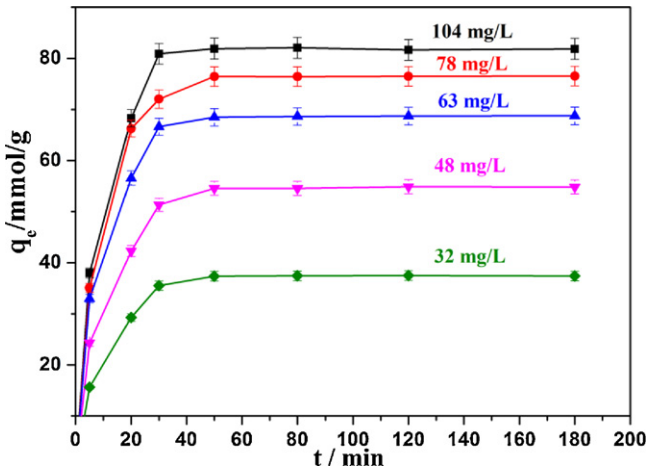

Fig. 10. Effects of reaction time on adsorption capacity: Cr(III) ions concentration (32, 48, 63, 78 and 104 mg/L); adsorbent dosage 0.2 g/L; temperature 25 °C; pH 6.0; and speed agitation 120 rpm.

To investigate the mechanism involved in the adsorption, the thermodynamic behaviors of Cr(III) ion adsorption onto the APTEOS/SA were evaluated employing the following equations:

$$K_d = \frac{(C_0 - C_e)}{C_e}\frac{V}{M} \quad (2)$$

$$\ln K_d = \frac{\Delta S^0}{R} - \frac{\Delta H^0}{RT} \quad (3)$$

$$\Delta G^0 = -RT \ln K_d \quad (4)$$

where K_d is the distribution coefficient (L g^{-1}), C_0 is the initial concentration (mg/L), ΔH^0 is the enthalpy change, ΔS^0 is the entropy change and ΔG^0 is the Gibbs free energy change in a given process (kJ/mol), respectively.

Thermodynamic parameters are calculated according to Eqs. (2)–(4) and shown in Table 1. ΔG^0 values negative for Cr(III) adsorption onto the APTEOS/SA indicate that the adsorption is spontaneous. These values decreased with an increase of temperature indicating a better adsorption performance was obtained at higher temperature. The positive values of ΔH^0 confirm the endothermic nature of the overall adsorption process. The positive value of ΔS^0 suggests an increased randomness at the solid/solution interface with some structural changes in the adsorbate and the adsorbent during the adsorption process.

3.6. Effect of reaction time on the adsorption behavior

The adsorption process could be controlled either by a chemical reaction or by diffusion, such as pore and film diffusion. Effects of reaction time on Cr(III) ions adsorption capacity are presented in Fig. 10. Increase in adsorption capacity with increasing contact time is ascribed to the fact that more time becomes available for Cr(III) ions to interact with the active functional groups on the APTEOS/SA. It also shows that the Cr(III) ions adsorption is rapid within the first 30 min, then increase slowly, and the adsorption process attained equilibrium within 50 min. Therefore, the adsorption experiments were conducted for 50 min, except the indicated. The initial Cr(III) ions adsorption rate by the APTEOS/SA is very high as a large number of adsorption sites are available for adsorption. Meanwhile, in the initial pristine surface of the APTEOS/SA, the sticking probability is large and consequently adsorption proceeds with a high rate. Once the available free surface is gradually filled up by the adsorbate species, adsorption process becomes slow and the kinetics may become more dependent on the rate at which the adsorbate

Table 1
Thermodynamic parameters calculated for the adsorption of Cr(III) ions onto the APTEOS/SA: adsorbent dose 0.2 g/L; Cr(III) ions concentration 63 mg/L; pH 6.0; speed agitation 120 rpm; and time 50 min.

Adsorbent	ΔH^0 (kJ/mol)	ΔS^0 (kJ/mol)	ΔG^0 (kJ/mol)					
			298.15 (k)	303.15 (k)	308.15 (k)	313.15 (k)	318.15 (k)	323.15 (k)
APTEOS/SA	4.662	0.183	0.797	0.866	0.952	1.041	1.158	1.251

Table 2
The Lagergren pseudo-first-order rate parameters for Cr(III) ions adsorption onto the APTEOS/SA: adsorbent dosage 0.2 g/L; temperature 25 °C; pH 6.0; speed agitation 120 rpm; and time 120 min.

Metal ions	C_0 (mg/L)	q_e (mg/g)	k_1 ($\times 10^{-2}$ min^{-1})	$q_{e,c}$ (mg/g)	R^2
Cr(III)	32	37.44	8.62	33.96	0.9927
	48	54.60	9.16	56.13	0.9976
	63	68.64	9.51	64.53	0.9958
	78	76.44	11.04	72.74	0.9913
	104	82.16	14.51	88.79	0.9970

molecules diffuse into the pore and get adsorbed on the surface of the inside pores.

3.7. Adsorption kinetics and isotherms study

3.7.1. Adsorption kinetics study

To examine the mechanism of adsorption processes, such as mass transfer and chemical reaction, we tested the Lagergren pseudo-first-order kinetic model and pseudo-second-order kinetic model, the intra-particular diffusion model and the Crank model [48,49] with our experimental data.

(1) Lagergren pseudo-first-order kinetic model:

$$\ln(q_e - q_t) = \ln q_e - k_1 t \tag{5}$$

(2) Pseudo-second-order kinetic model:

$$\frac{t}{q_t} = \left(\frac{1}{k_2 q_e^2}\right) + \frac{t}{q_e} \tag{6}$$

where q_e and q_t denote the amounts of adsorption per unit mass of the adsorbent at equilibrium and at time t (mg/g) and k_1 and k_2 are the first order and second order rate constants (min^{-1}), respectively.

The amount of adsorption equilibrium q_e, the rate constants of the equation (l/min), k_1 and k_2, the calculated amount of adsorption equilibrium, $q_{e,c}$, and the coefficient of determination, R^2 are shown in Tables 2 and 3, respectively. From Tables 2 and 3, we found that the pseudo-first-order equation appears to be the better-fitting model because it has the higher R^2. Meanwhile, the calculated amount of adsorption equilibrium ($q_{e,c}$) from pseudo-second-order equation is close to the actual amount of adsorption equilibrium (q_e).

(3) Intra-particular diffusion model:

$$q_t = k_{dif} t^{1/2} + C \tag{7}$$

Table 3
The Lagergren pseudo-second-order rate parameters for Cr(III) ions adsorption onto the APTEOS/SA: adsorbent dosage 0.2 g/L; temperature 25 °C; pH 6.0; speed agitation 120 rpm; and time 120 min.

Metal ions	C_0 (mg/L)	q_e (mg/g)	k_2 ($\times 10^{-3}$ min^{-1})	$q_{e,c}$ (mg/g)	R^2
Cr(III)	32	37.44	2.51	44.05	0.9665
	48	54.60	1.87	64.47	0.9823
	63	68.64	1.75	78.68	0.9743
	78	76.44	1.65	87.95	0.9678
	104	82.16	1.46	95.15	0.9889

where q_t is the amount of adsorption per unit of adsorbent at time t (mg/g), and k_{dif} is the intra-particular diffusion rate constant (mg g^{-1} min$^{-1/2}$).

The relation plots of q_t versus time $t^{1/2}$ are shown in Fig. 11. It shows that the plots are not linear over the whole time range and can be separated into two linear regions which confirm the multi-stages of adsorption. It may be concluded that surface adsorption and intra-particle diffusion were concurrently happened in the present study. The first stage is characterized by physical adsorption of the APTEOS/SA functional groups and the second stage is due to the intra-particle diffusion effects [50].

(4) Crank model:

According to Crank diffusion model, the mass transfer rate of the Cr(III) ions, N_t, at the external surface of the adsorbent can be described as follows:

$$N_t = \frac{\partial C_t}{\partial t} = k_f S_A (C_t - C_s) \tag{8}$$

where C_t is bulk liquid phase concentration (mg/L), C_s is liquid phase concentration at the surface in equilibrium with the solid phase concentration (mg/L), k_f is an external mass transfer coefficient (m/s), and S_A is the specific surface area of adsorbent (m^2/g).

Integrating Eq. (8), the following expression is obtained:

$$\ln\left(\frac{C_t}{C_0}\right) = -k_f S_A t \tag{9}$$

Crank also developed the following equation for a slab particle [51]:

$$\frac{q_t}{q_e} = 1 - \sum_{n=1}^{\infty} \frac{6}{\pi^2 n^2} \times \exp\left(\frac{-n^2 \pi^2 D_S t}{r^2}\right) \tag{10}$$

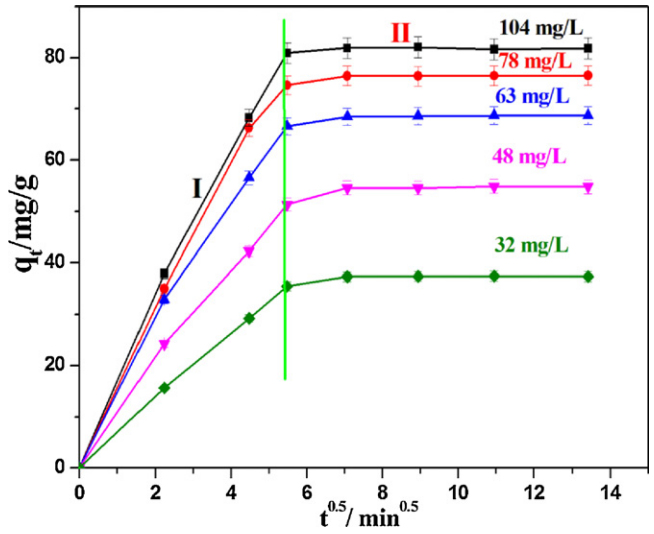

Fig. 11. Investigate intra-particular diffusion model for Cr(III) ions adsorption on the APTEOS/SA (Cr(III) ions concentration (32, 48, 63, 78 and 104 mg/L); adsorbent dosage 0.2 g/L; temperature 25 °C; pH 6.0; and speed agitation 120 rpm.).

Table 4
Kinetic data from the Crank model and Biot number: adsorbent dosage 0.2 g/L; temperature 25 °C; pH 6.0; speed agitation 120 rpm; and time 120 min.

Metal ions	C_0 (mg/L)	k_f ($\times 10^{-5}$ m/s)	D_S ($\times 10^{-12}$ m^2/s)	Biot
Cr(III)	32	1.63	3.02	108
	48	1.67	3.21	104
	63	1.72	3.85	91
	78	1.75	4.03	88
	104	1.80	4.67	77

where D_S is the effective intra-particle diffusion coefficient of the adsorbent in the particle (m^2/s).

The Biot number, B_i (dimensionless), could be calculated as below:

$$B_i = \frac{k_f L_f}{D_S} \quad (11)$$

where, L_f is the thickness of the film.

The B_i values calculated with experimental data are presented in Table 4. It was observed that all the B_i values were significantly higher than one, which suggested that the adsorption process was mainly controlled by the intra-particle diffusion [51].

3.7.2. Adsorption isotherms study

In an adsorption system, the adsorption results in the removal of solute from the solution onto the adsorbent surface until the remaining solute in the solution is in dynamic equilibrium with solute on the adsorbent surface. A plot of the solute concentration in the adsorbent phase q_e (mg/g) as function of the solute concentration in the solution C_e (mg/L) at equilibrium gives an adsorption isotherm. An adsorption isotherm can be utilized to obtain information about the interaction between the adsorbent and adsorbate molecules. In order to understand and clarify the adsorption process, Langmuir adsorption isotherm and Freundlich adsorption isotherm models were applied in this study.

The Langmuir adsorption isotherm equation is an often used adsorption model of completely homogenous surface with negligible interaction between adsorbed molecules, shown as below:

$$\frac{C_e}{q_e} = \frac{1}{bq_{\max}} + \frac{C_e}{q_{\max}} \quad (12)$$

where q_e is the amount of adsorption at equilibrium (mg/g), C_e is the equilibrium concentration of the adsorbate in the solution (mg/L). $q_{\max}$ is the adsorption capacity (mg/g), and b is the adsorption intensity or Langmuir coefficient related to the affinity of the binding site (L/mg).

The Freundlich adsorption isotherm equation is a purely empirical relationship based on heterogeneous surfaces suggesting that binding sites are not equivalent and independent. The Freundlich adsorption isotherm equation can be expressed as follows:

$$\ln q_e = \ln K_F + \frac{1}{n} \ln C_e \quad (13)$$

where K_F and $1/n$ are the constants that are related to the adsorption capacity and the adsorption intensity, respectively. A smaller $1/n$ value indicates a more heterogeneous surface whereas a value closer to or equal to one indicates the adsorbent has relatively more homogeneous binding sites.

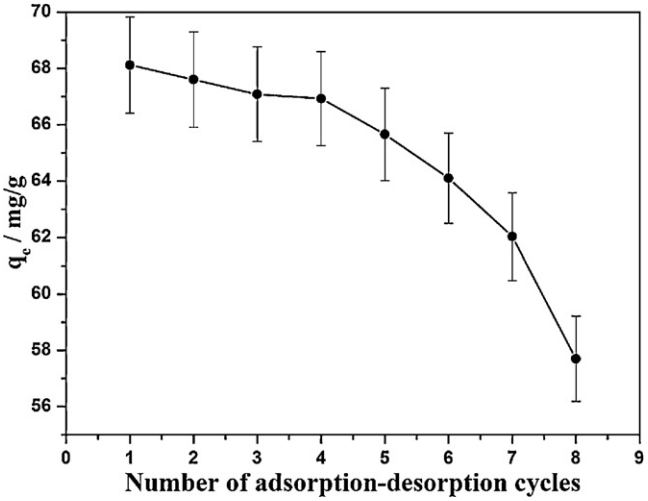

Fig. 12. The reusability of APTEOS/SA for removal of Cr(III) ions (desorption medium 1.0 M HCl 250 mL; Cr(III) ions concentration 78 mg/L; adsorbent dosage 0.2 g/L; temperature 25 °C; speed agitation of 120 rpm; and time 120 min).

The isotherm constants were calculated from the experimental data and presented in Table 5. Taking into consideration the values of the correlation coefficient as a criterion for goodness of fit for the system, the Freundlich isotherm model shows better correlation (R^2 = 0.9834) than the Langmuir isotherm model (R^2 = 0.9163), which indicated that the Freundlich adsorption isotherm model represented the adsorption process more ideally. It also suggested the heterogeneous nature of adsorptive sites on the surface of the APTEOS/SA.

3.8. Desorption of heavy metal ions and reusability

Reusability is an important factor for an adsorbent because it will reduce the overall cost of the applied adsorbent. To evaluate the reusability of the adsorbent, we carried out the consecutive adsorption–desorption process for five times. Just as Fig. 12 indicated that the total adsorption capacity of the PTEOS/SA for Cr(III) ions after eight cycles decreased slightly from 68.1 to 57.7 mg/g, not more than 16.0%. The adsorption–desorption results indicated that the prepared APTEOS/SA could be used effectively for treatment wastewater containing low concentration Cr(III) ions.

4. Discussion and conclusion

In this study, a novel porous membrane adsorbent 3-aminopropyl-triethoxysilane functionalized sodium alginate was prepared, and some important parameters affected the adsorption behavior of the APTEOS/SA for Cr(III) ions from aqueous solutions were also tested. The adsorption capacity of the APTEOS/SA for Cr(III) ions was highly pH-dependent, and the best adsorption capacity could be obtained at solution pH 6.0. Adsorption capacity of the APTEOS/SA was also temperature-dependent, an increase in temperature enhanced adsorption capacity of the APTEOS/SA for Cr(III) ions. The adsorption rate was fast and adsorption equilibrium was obtained within 50 min. The maximum uptake capacity of the APTEOS/SA for Cr(III) ions under the optimal condition

Table 5
Kinetic data from the Langmuir isotherm and the Freundlich isotherm: adsorbent dosage 0.2 g/L; temperature 25 °C; pH 6.0; speed agitation 120 rpm; and time 50 min.

Metals ion	Langmuir, $q_{\max}$ (mg/g)	Isotherm, b (L/mg)	Parameters, R^2	Freundlich, K_F (mg/g)	Isotherm, n	Parameters, R^2
Cr(III)	116.41	0.887	0.9163	5.98	1.61	0.9834

was 90.0 mg/g. The FT-IR, SEM-EDX, TG, AFM, and contact angle goniometer methods were efficient techniques for investigating the physico-chemical characters of the pristine and Cr(III) ions loaded APTEOS/SA. The kinetics adsorption data could be well fitted with pseudo-first-order kinetic model. Meanwhile, the kinetic experiment results also indicated that the rate of controlling step was mainly intra-particle diffusion but was not the only rate-limiting step for Cr(III) ions adsorption. The equilibrium data can be well fitted with the Freundlich isotherm model. The successive adsorption–desorption experiment indicated that 1.0 M HCl could be effectively used for desorption of Cr(III) ion from the APTEOS/SA. The prepared APTEOS/SA can be used for removing Cr(III) ions from the aqueous solution with high reusability.

Acknowledgements

The authors would like to acknowledge the financial support of this work from National Natural Science Foundation of China (No. 21076174). The authors also thank the anonymous referees for comments on this manuscript.

References

[1] L. Bai, H.P. Hua, W. Fu, J. Wan, X.L. Cheng, L.Z. Ge, L. Xiong, Q.Y. Chen, Synthesis of a novel silica-supported dithiocarbamate adsorbent and its properties for the removal of heavy metal ions, J. Hazard. Mater. 195 (2011) 261–275.
[2] Z. Li, Q. Tang, T. Katsumi, X.W. Tang, T. Inui, S. Imaizumi, Leaf char: an alternative adsorbent for Cr(III), Desalination 264 (2010) 70–77.
[3] M. Kebir, M. Chabani, N. Nasrallah, A. Bensmaili, M. Trari, Coupling adsorption with photocatalysis process for the Cr(VI) removal, Desalination 270 (2011) 166–173.
[4] P. Suksabye, P. Thiravetyan, Cr(VI) adsorption from electroplating plating wastewater by chemically modified coir pith, J. Environ. Manage. 102 (2012) 1–8.
[5] P. Miretzky, A. Fernandez Cirelli, Cr(VI) and Cr(III) removal from aqueous solution by raw and modified lignocellulosic materials: a review, J. Hazard. Mater. 180 (2010) 1–19.
[6] A. Esayas, T.B. Sören, L. Bernd, Adsorption behaviour of Cr(VI) onto macro and micro-vesicular volcanic rocks from water, Sep. Purif. Technol. 78 (2011) 55–61.
[7] Q. Wang, J.Y. Song, M.Z. Sui, Characteristic of adsorption, desorption and oxidation of Cr(III) on birnessite, Energy Procedia 5 (2011) 1104–1108.
[8] M. Ciopec, C.M. Davidescu, A. Negrea, I. Grozav, L. Lupa, P. Negrea, A. Popa, Adsorption studies of Cr(III) ions from aqueous solutions by DEHPA impregnated onto Amberlite XAD7–Factorial design analysis, Chem. Eng. Res. Des. 90 (2012) 1660–1670.
[9] Q.H. Wang, X.J. Chang, D.D. Li, Z. Hu, R.J. Li, Q. He, Adsorption of chromium(III), mercury(II) and lead(II) ions onto 4-aminoantipyrine immobilized bentonite, J. Hazard. Mater. 186 (2011) 1076–1081.
[10] S.K. Yahy, Z.A. Zakaria, J. Samin, A.S. Santhana Raj, W.A. Ahmad, Isotherm kinetics of Cr(III) removal by non-viable cells of *Acinetobacter haemolyticus*, Colloids Surf. B 94 (2012) 362–368.
[11] X. Huang, X.P. Liao, B. Shi, Tannin-immobilized mesoporous silica bead (BT-SiO_2) as an effective adsorbent of Cr(III) in aqueous solutions, J. Hazard. Mater. 173 (2010) 33–39.
[12] A. Lodi, D. Soletto, C. Solisio, A. Converti, Chromium(III) removal by *Spirulina platensis* biomass, Chem. Eng. J. 136 (2008) 151–155.
[13] Y.T. He, S.J. Traina, Cr(VI) reduction and immobilization by magnetite under alkaline pH conditions: the role of passivation, Environ. Sci. Technol. 39 (2005) 4499–4504.
[14] F.J. Alguacil, M. Alonso, F. Lopez, A.L. Delgado, Uphill permeation of Cr(VI) using Hostarex A327 as ionophore by membrane-solvent extraction processing, Chemosphere 72 (2008) 684–689.
[15] K.Y. Wang, T.S. Chung, Fabrication of polybenzimidazole (PBI) nanofiltration hollow fiber membranes for removal of chromate, J. Membr. Sci. 281 (2006) 307–315.
[16] M.M. Nasef, A.H. Yahaya, Adsorption of some heavy metal ions from aqueous solutions on Nafion 117 membrane, Desalination 249 (2009) 677–681.
[17] Y.H. Liu, L. Guo, J. Chen, Removal of Cr(III, VI) by quaternary ammonium and quaternary phosphonium ionic liquids functionalized silica materials, Chem. Eng. J. 158 (2010) 108–114.
[18] M. Hamdi Karaoğlu, S. Zor, M. Uğurlu, Biosorption of Cr(III) from solutions using vineyard pruning waste, Chem. Eng. J. 159 (2010) 98–106.
[19] X.H. Zou, J.M. Pan, H.X. Ou, X. Wang, W. Guan, C.X. Li, Y.S. Yan, Y.Q. Duan, Adsorptive removal of Cr(III) and Fe(III) from aqueous solution by chitosan/attapulgite composites: equilibrium, thermodynamics and kinetics, Chem. Eng. J. 167 (2011) 112–121.
[20] F.Q. An, B.J. Gao, Adsorption characteristics of Cr(III) ionic imprinting polyamine on silica gel surface, Desalination 249 (2009) 1390–1396.
[21] J.H. Chen, G.P. Li, Q.L. Liu, J.C. Ni, W.B. Wu, J.M. Lin, Cr(III) ionic imprinted polyvinyl alcohol/sodium alginate (PVA/SA) porous composite membranes for selective adsorption of Cr(III) ions, Chem. Eng. J. 165 (2010) 465–473.
[22] G.J. Copello, L.E. Diaz, V.C. Dall'Orto, Adsorption of Cd(II) and Pb(II) onto a one step-synthesized polyampholyte: kinetics and equilibrium studies, J. Hazard. Mater. 217/218 (2012) 374–381.
[23] A. Shahbazi, H. Younesi, A. Badiei, Functionalized SBA-15 mesoporous silica by melamine-based dendrimer amines for adsorptive characteristics of Pb(II) Cu(II) and Cd(II) heavy metal ions in batch and fixed bed column, Chem. Eng. J. 168 (2011) 505–518.
[24] M. Pansini, C. Colella, D. Caputo, M. de'Gennaro, A. Langella, Evaluation of phillipsite as cation exchanger in lead removal from water, Microporous Mater. 5 (1996) 357–364.
[25] A. Langella, M. Pansini, P. Cappelletti, B. De Gennaro, M. De' Gennaro, C. Colella, NH_4^+, Cu^{2+}, Zn^{2+}, Cd^{2+} and Pb^{2+} exchange for Na^+ in a sedimentary clinoptilolite, Microporous Mesoporous Mater. 37 (2000) 337–343.
[26] M. Mercurio, V. Mercurio, B. de' Gennaro, M. de' Gennaro, C. Grifa, A. Langella, V. Morra, Natural zeolites and white wines from Campania region (Southern Italy): a new contribution for solving some oenological problems, Per. Mineral. 79 (2010) 95–112.
[27] S. Kalidhasan, A.S.K. Kumar, V. Rajesh, N. Rajesh, Ultrasound-assisted preparation and characterization of crystalline cellulose–ionic liquid blend polymeric material: a prelude to the study of its application toward the effective adsorption of chromium, J. Colloid Interface Sci. 367 (2012) 398–408.
[28] Y.M. Zhou, Q. Jin, T.W. Zhu, Y. Akama, Adsorption of chromium(VI) from aqueous solutions by cellulose modified with β-CD and quaternary ammonium groups, J. Hazard. Mater. 187 (2011) 303–310.
[29] G.R. Xie, X.Q. Shang, R.F. Liu, J. Hu, S.F. Liao, Synthesis and characterization of a novel amino modified starch and its adsorption properties for Cd(II) ions from aqueous solution, Carbohydr. Polym. 84 (2011) 430–438.
[30] C.L. Dai, Y.J. Wang, X. Hou, Preparation and protein adsorption of porous dextran microspheres, Carbohydr. Polym. 87 (2012) 2338–2343.
[31] C. Demirbilek, C. Dincs, Synthesis of diethylaminoethyl dextran hydrogel and its heavy metal ion adsorption characteristics, Carbohydr. Polym. 90 (2012) 1159–1167.
[32] G.Z. Kyzas, M. Kostoglou, A.A. Vassiliou, N.K. Lazaridis, Treatment of real effluents from dyeing reactor: experimental and modeling approach by adsorption onto chitosan, Chem. Eng. J. 168 (2011) 577–585.
[33] A. Ghaee, M.S. Niassar, J. Barzinc, A. Zarghan, Adsorption of copper and nickel ions on macroporous chitosan membrane: equilibrium study, Appl. Surf. Sci. 258 (2012) 7732–7743.
[34] A.T. Paulino, L.A. Belfiore, L.T. Kubot, E.C. Muniz, V.C. Almeida, E.B. Tambourgi, Effect of magnetite on the adsorption behavior of Pb(II), Cd(II), and Cu(II) in chitosan-based hydrogels, Desalination 275 (2011) 187–196.
[35] P. Agrawal, R. Patil, N. Kalyaneb, U.V.A. Joshi, Formulation and in-vitro evaluation of zidovudine loaded calcium alginate microparticles containing copolymer, J. Pharm. Res. 3 (2010) 486–490.
[36] S. Galus, A. Lenart, Development and characterization of composite edible films based on sodium alginate and pectin, J. Food Eng. (2012), http://dx.doi.org/10.1016/j.jfoodeng.2012.03.006
[37] L.L. Yang, X.Y. Ma, N.N. Guo, Sodium alginate/Na^+-rectorite composite microspheres: preparation, characterization, and dye adsorption, Carbohydr. Polym. 90 (2012) 853–858.
[38] E.S. Abdel-Halima, S.S. Al-Deyab, Removal of heavy metals from their aqueous solutions through adsorption onto natural polymers, Carbohydr. Polym. 84 (2011) 454–458.
[39] J.H. Chen, Q.L. Liu, S.R. Hu, J.C. Ni, Y.S. He, Adsorption mechanism of Cu(II) ions from aqueous solution by glutaraldehyde crosslinked humic acid-immobilized sodium alginate porous membrane adsorbent, Chem. Eng. J. 173 (2011) 511–519.
[40] X.L. Li, Y.F. Li, Z.F. Ye, Preparation of macroporous bead adsorbents based on poly(vinylalcohol)/chitosan and their adsorption properties for heavy metals from aqueous solution, Chem. Eng. J. 178 (2011) 60–68.
[41] N.N. Jiang, Y.T. Xu, Y.Q. Dai, W.A. Luo, L.Z. Dai, Polyaniline nanofibers assembled on alginate microsphere for Cu^{2+} and Pb^{2+} uptake, J. Hazard. Mater. 215/216 (2012) 17–24.
[42] E. Repo, J.K. Warchoł, A. Bhatnagar, M. Sillanpää, Heavy metals adsorption by novel EDTA-modified chitosan–silica hybrid materials, J. Colloid Interface Sci. 358 (2011) 261–267.
[43] A.D. Eaton, L.S. Clesceri, A.E. Greenberg, Standard Methods for the Examination of Water and Wastewater, 20th edition, American Public Health Association, Washington, DC, 1999.
[44] E. Broderick, H. Lyons, T. Pembroke, H. Byrne, B. Murray, M. Hall, The characterisation of a novel, covalently modified, amphiphilic alginate derivative, which retains gelling and non-toxic properties, J. Colloid Interface Sci. 298 (2006) 154–161.
[45] X.H. Wang, M. Han, J.C. Bao, W.W. Tu, Z.H. Dai, A superoxide anion biosensor based on direct electron transfer of superoxide dismutase on sodium alginate sol–gel film and its application to monitoring of living cells, Anal. Chim. Acta 717 (2012) 61–66.
[46] J. Samuel, M. Pulimi, M.L. Paul, A. Maurya, N. Chandrasekaran, A. Mukherjee, Batch and continuous flow studies of adsorptive removal of Cr(VI) by adapted bacterial consortia immobilized in alginate beads, Bioresour. Technol. 128 (2013) 423–430.

[47] P. Lodeiro, A. Fuentes, R. Herrero, M.E. Sastre de Vicente, Cr(III) binding by surface polymers in natural biomass: the role of carboxylic groups, Environ. Chem. 5 (2008) 355–365.
[48] Y.S. Ho, Review of second-order models for adsorption systems, J. Hazard. Mater. B136 (2006) 681–689.
[49] C.O. Illanes, N.A. Ochoa, J. Marchese, Kinetic sorption of Cr(VI) into solvent impregnated porous microspheres, Chem. Eng. J. 136 (2008) 92–98.
[50] M.A. Tofighy, T. Mohammadi, Adsorption of divalent heavy metal ions from water using carbon nanotube sheets, J. Hazard. Mater. 185 (2011) 140–147.
[51] P.W. Majsztrik, M.B. Satterfield, A.B. Bocarsly, J.B. Benziger, Water sorption, desorption and transport in Nafion membranes, J. Membr. Sci. 301 (2007) 93–106.